

ORIGINAL ARTICLE

Efficient and stable transduction of dopaminergic neurons in rat substantia nigra by rAAV 2/1, 2/2, 2/5, 2/6.2, 2/7, 2/8 and 2/9

A Van der Perren¹, J Toelen², M Carlon², C Van den Haute¹, F Coun¹, B Heeman¹, V Reumers¹, LH Vandenberghe³, JM Wilson³, Z Debyser² and V Baekelandt¹

Dysfunction of the nigrostriatal system is the major cause of Parkinson's disease (PD). This brain region is therefore an important target for gene delivery aiming at disease modeling and gene therapy. Recombinant adeno-associated viral (rAAV) vectors have been developed as efficient vehicles for gene transfer into the central nervous system. Recently, several serotypes have been described, with varying tropism for brain transduction. In light of the further development of a viral vector-mediated rat model for PD, we performed a comprehensive comparison of the transduction and tropism for dopaminergic neurons (DNs) in the adult Wistar rat substantia nigra (SN) of seven rAAV vector serotypes (rAAV 2/1, 2/2, 2/5, 2/6.2, 2/7, 2/8 and 2/9). All vectors were normalized by titer and volume, and stereotactically injected into the SN. Gene expression was assessed non-invasively and quantitatively *in vivo* by bioluminescence imaging at 2 and 5 weeks after injection, and was found to be stable over time. Immunohistochemistry at 6 weeks following injection revealed the most widespread enhanced green fluorescence protein expression and the highest number of positive nigral cells using rAAV 2/7, 2/9 and 2/1. The area transduced by rAAV 2/8 was smaller, but nevertheless almost equal numbers of nigral cells were targeted. Detailed confocal analysis revealed that serotype 2/7, 2/9, 2/1 and 2/8 transduced at least 70% of the DN. In conclusion, these results show that various rAAV serotypes efficiently transduce nigral DN, but significant differences in transgene expression pattern and level were observed. Gene Therapy advance online publication, 17 February 2011; doi:10.1038/gt.2010.179

Keywords: adeno-associated viral vectors; dopaminergic neurons; substantia nigra; *in vivo* bioluminescence imaging; Parkinson's disease

INTRODUCTION

Parkinson's disease (PD) is a neurodegenerative movement disorder characterized by a progressive loss of dopaminergic neurons (DNs) in the substantia nigra pars compacta (SNpc). This cell loss results in striatal depletion of dopamine that modulates the initiation of voluntary movements. Although the exact etiology and the molecular pathogenesis of the disease remain unclear, a combination of multiple genetic and environmental factors in the context of an ageing brain is involved. Recently, significant progress has been made in the identification of genes that are responsible for monogenetic forms of PD.^{1–5} Some of these genes offer new possibilities for disease modeling,^{6–10} while others are promising candidates for targeted (gene) therapy.^{11–13}

Experimental models of PD are indispensable tools in preclinical research, both for the elucidation of the disease mechanisms and for the development of novel therapeutics. These models are based on toxicological, transgenic or viral vector-based stereotactic gene delivery approaches. Injection of toxins such as 6-hydroxydopamine,¹⁴ MPTP,¹⁵ pesticides¹⁶ or herbicides¹⁷ efficiently induces specific loss of DN, and can be applied in multiple species at different developmental time points. The use of transgenic mouse models has been instrumental in dissecting the pathophysiology of PD.^{18–22} These models

are, however, restricted to a single species, are often limited in specific targeting of the nigrostriatal pathway and, in general, lack controlled transgene expression. Viral vector-mediated gene delivery combines the advantages of the toxicological and transgenic models, as it enables researchers to induce transgene expression in the central nervous system (CNS) in a site- and time-specific manner in multiple species.²³ Recombinant adenoviral, retroviral, lentiviral and adeno-associated viral (rAAV) vectors have been used in the CNS. The brain parenchyma consists of different cell types, such as neurons, astrocytes, microglia, oligodendroglia and epithelial cells, which may be differentially transduced by different viral vectors. In the context of preclinical PD research, the DN of the SNpc are the main targets for gene delivery. Both lentiviral and rAAV vectors have been used to deliver transgenes into the nigrostriatal system for purposes of disease modeling^{6–10,24} or gene therapy.^{12,25} rAAV vectors are particularly attractive for targeting the substantia nigra (SN)^{26–32} because of their high titers and tropism for neurons, while inducing minimal immune responses in the brain. rAAV vectors are derived from a 4.7-kb single-stranded DNA virus that belongs to the family of the parvoviridae. To date, the most widely used rAAV vector is based on the AAV2 serotype, and has been successfully used in mammalian brain, where

¹Neurobiology and Gene Therapy, Molecular Medicine, Katholieke Universiteit Leuven, Flanders, Belgium; ²Molecular Virology and Gene Therapy, Molecular Medicine, Katholieke Universiteit Leuven, Flanders, Belgium and ³Gene Therapy Program, Department of Pathology and Laboratory Medicine, Division of Transfusion Medicine, University of Pennsylvania, Philadelphia, PA, USA

Correspondence: Professor V Baekelandt, Neurobiology and Gene Therapy, Molecular Medicine, Katholieke Universiteit Leuven, Kapucijnenvoer 33, VCTB+5, Leuven, Flanders B-3000, Belgium.

E-mail: Veerle.Baekelandt@med.kuleuven.be

Received 20 July 2010; revised 19 December 2010; accepted 21 December 2010

mainly neurons are targeted.³³ A drawback of rAAV 2/2, however, is that for some brain regions only a relatively small volume is transduced.^{29,34} Recent advances in rAAV vector technology have increased the number of applications of this vector system. These modifications include the development of improved scaled manufacturing, the isolation of novel serotypes, the possibility of cross-packaging and the testing of functional control elements (promoters, post-transcriptional regulatory elements and so on), which enhance transgene expression and stability.^{35–39} The availability of novel serotypes may also improve specific neural targeting and vector distribution in the brain.^{27–31}

In this comparative study, we have evaluated the tropism and transduction efficiency over time of rAAV vector serotypes 2/1, 2/2, 2/5, 2/6.2, 2/7, 2/8 and 2/9 after stereotactic injection in the SN of the adult rat brain. We have characterized transgene expression by non-invasive bioluminescence imaging (BLI) and by immunohistochemical (IHC) analysis of the total transduced brain volume, as well as at the dopaminergic cell level. The most suitable rAAV vector should ideally transduce the highest number of dopaminergic cells covering the entire SN. Our findings will facilitate the design and selection of rAAV serotypes for transduction of the SN tailored to specific research needs.

RESULTS

Quantification of transgene expression after injection of different rAAV serotypes in rat SN by non-invasive BLI

Preparations of rAAV serotypes 2/1, 2/5, 2/6.2, 2/7, 2/8 or 2/9 were normalized by titer and volume (1.0×10^{10} GC ml⁻¹, injected titer 3.0×10^7 GC per animal), and stereotactically injected into rat SN. In order to compare all serotypes with rAAV 2/2, we produced this serotype once from the cell lysate and once from the supernatant. Whereas the other serotypes were efficiently produced from the supernatant, production of rAAV 2/2 is more efficient from cell lysates.^{40–42} The rAAV 2/2 vectors were also injected in the SN (1.0×10^{10} GC ml⁻¹, injected titer 3.0×10^7 GC per animal). *In vivo* BLI was used to non-invasively assess the levels and kinetics of transgene expression in each of the injected animals (Figure 1a). The animals were scanned 2 weeks and 5 weeks after intranigral injection. Quantification of the *in vivo* BLI signal indicated stable firefly luciferase (fLuc) expression over time. No significant differences were observed between the two time points for any serotype ($P > 0.05$) (Figure 1b). The highest BLI signal was observed with rAAV 2/7, which was 10 times higher than with rAAV 2/9 and 2/1, and 50–100 times higher than with rAAV 2/8, 2/5, 2/6.2 and 2/2 ($P < 0.05$).

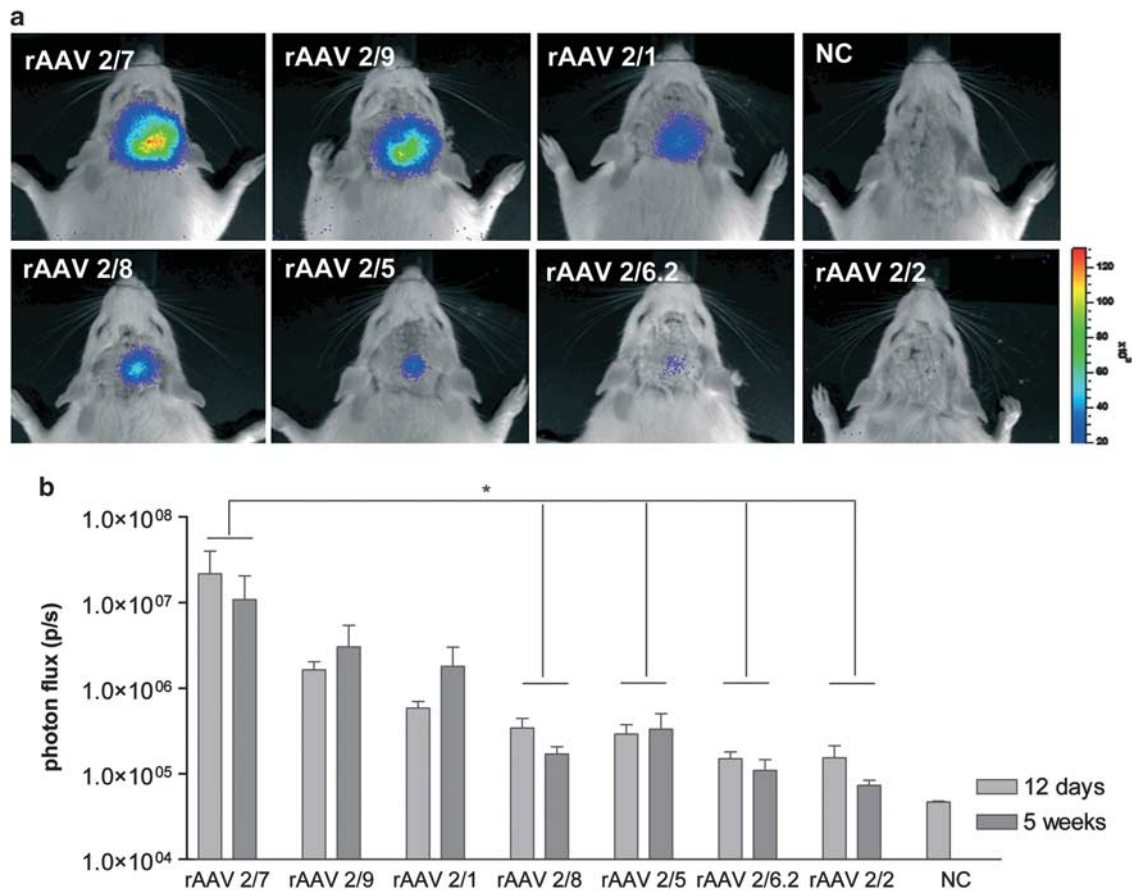


Figure 1 *In vivo* BLI of transgene expression after injection of rAAV serotypes in the rat SN. (a) BLI signal in overlay with a photographic image of the rat head region. Two weeks after injection, a light signal originating from the site of injection (SN) was detected. The pseudocolor scale depicts the photon flux per second, per square centimeter per steradian ($\text{ps}^{-1} \text{cm}^{-2} \text{sr}^{-1}$). Measurements were obtained in a 3.0-cm^2 circular region of interest on the head. (b) *In vivo* BLI quantification of fLuc transgene expression in the rat brain. fLuc activity was measured 2 weeks and 5 weeks after stereotactic injection of different rAAV serotypes. The highest BLI signal was observed with rAAV 2/7. This signal was significantly higher than with rAAV 2/8, 2/5, 2/6.2 and 2/2 (mean \pm s.d., * $P < 0.05$, $n = 5$). Note, for rAAV 2/2 the vector was produced from the cell lysate.

Measurement of transduced brain volume after injection of rAAV vectors in the rat SN

We determined transduction efficiency by IHC staining for enhanced green fluorescent protein (eGFP) 6 weeks after injection. Distinct expression patterns were apparent for the different serotypes (Figure 2a). The transduced volume for each serotype was quantified stereologically with the Cavalieri method (Figure 2b). Injection of rAAV 2/7, 2/9 and 2/1 resulted in widespread transgene expression ($>20\text{ mm}^3$). The volume transduced by rAAV 2/8, rAAV 2/5 and rAAV 2/6.2 ranged from 6 to 10 mm^3 , which was significantly lower ($P<0.001$). The transduced volume of rAAV 2/2 was only 1.5 mm^3 ($P<0.001$).

Characterization of transduced cells after injection of rAAV vectors in the rat SN

Next, we determined the number of transduced cells in the SNpc using the optical fractionator method. The SN was delineated, and within this region monoaminergic neuronal cell types were distinguished from the smaller interneurons and glial cells based on their size and morphology. These nigral monoaminergic neuronal cells will henceforth be referred to as nigral cells. rAAV 2/7, 2/9 and 2/1 transduced the highest number of nigral cells, covering nearly the entire SN (Figure 2c). Despite the lower total transduced brain volume, rAAV 2/8 transduced an equal number of nigral cells, while rAAV 2/5, 2/6.2 and 2/2 transduced a significantly lower number of nigral cells

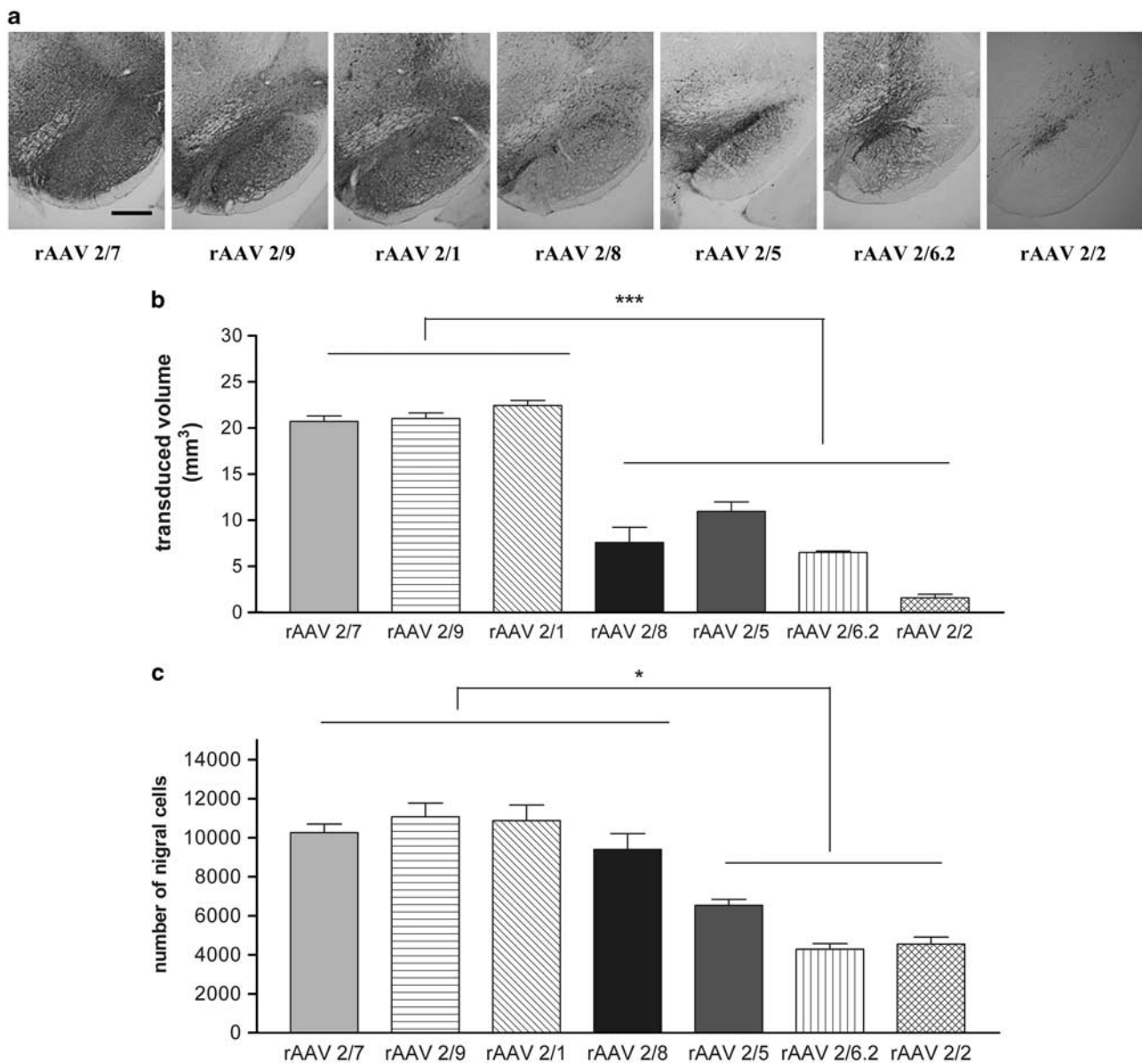


Figure 2 Transduction of rat SN with different rAAV serotypes. (a) IHC staining for eGFP 6 weeks after rAAV injection in SN. Scale bar=400µm. (b) Quantification of the transduced volume. The volume transduced by each rAAV serotype after intranigral injection of 3.0×10^7 GC was measured stereologically. Equivalent transduction volumes were observed for rAAV 2/7, 2/9 and 2/1. The volume transduced by rAAV 2/5, 2/8, 2/6.2 and 2/2 was significantly lower (mean \pm s.d., $***P<0.001$, $n=4$). (c) Quantification of the number of transduced nigral cells in the SN. The number of transduced nigral cells was quantified stereologically. rAAV 2/7, 2/9, 2/1 and 2/8 transduced the highest number of nigral cells, while rAAV 2/5, 2/6.2 and 2/2 transduced a significantly lower number of nigral cells (mean \pm s.d., $*P<0.05$, $n=4$).

($P < 0.05$). To verify if cell loss occurred after injection of the different serotypes, we determined the number of DN_s using the dopaminergic marker tyrosine hydroxylase (TH). No differences were detected in the number of TH-positive cells for all tested serotypes (Supplementary Figure S1).

To compare the specific transduction efficiency of each rAAV serotype for DN_s, double staining for eGFP and the TH was

performed. Detailed confocal microscopic analysis and quantification in the transduced region showed a distinct co-localization of eGFP and TH, depending on the analyzed serotype (Figure 3a). Serotypes 2/7, 2/9, 2/1 and 2/8 transduced the largest proportion of DN_s in the transduced region ($> 70\%$), which was significantly higher than rAAV 2/5 or 2/6.2 (49%; $P < 0.01$) (Figure 3b). Taking into account the percentage and total number of transduced nigral cells, we conclude

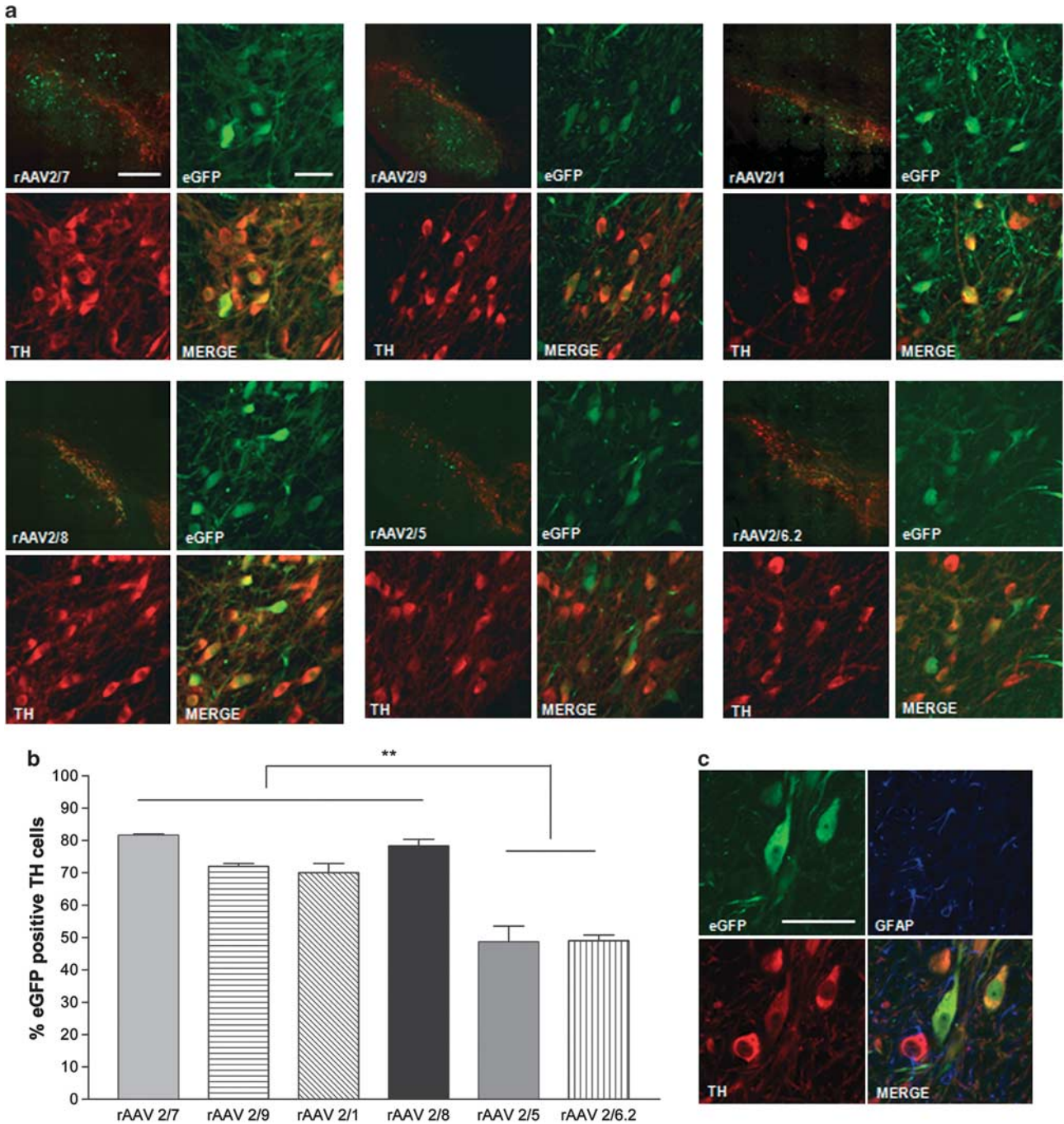


Figure 3 Characterization of the cell types transduced by rAAV serotypes in the SN. (a) Confocal images of fluorescent double immunostainings for eGFP and TH show extensive co-localization in the transduced region. Scale bar=500 μ m (overview picture left on top), 50 μ m (detail pictures). (b) Quantification of the number of transduced DN_s in the SN. rAAV 2/7, 2/9, 2/1 and 2/8 transduced the highest number of DN_s, while rAAV 2/5 and 2/6.2 transduced significantly less DN_s (mean \pm s.d., $**P < 0.01$, $n=3$). (c) Confocal images of fluorescent triple immunostaining for eGFP, TH and GFAP show excellent co-localization between eGFP and TH, and an apparent absence of transduction of astrocytes. Scale bar=50 μ m.

that rAAV 2/7, 2/9, 2/1 and 2/8 result in the highest transduction efficiency of DN in the SN. rAAV 2/5 and 2/6.2 are less efficient compared with the other serotypes. Co-staining for the glial cell marker glial fibrillary acidic protein (GFAP) was minimal for all serotypes tested (Figure 3c), indicating inefficient transduction of astrocytes. GFAP immunostaining also revealed the absence of pronounced astrogliosis at 12 days or 6 weeks after injection (data not shown). Gliosis was apparent only near the injection tract, suggesting a low inflammatory response after rAAV vector transduction despite high and widespread transgene expression.

Comparison of the CMV and the enhanced synapsin1 promoter in rAAV vectors

As the specificity is determined not only by the serotype but also by the promoter driving transgene expression, we decided to compare transgene expression driven by two different promoters. Although all rAAV serotypes tested showed high dopaminergic specificity with the human cytomegalovirus (CMV) promoter, we also tested the enhanced human synapsin1 promoter, which may differ in terms of silencing or cell-type-specific activity. The small, 495-bp human synapsin1 promoter has been shown to drive neuron-specific expression.⁴³ The regulation of neuronal specificity of synapsin1 is accomplished by the neuron-restrictive silencer factor (NRSF)-binding motif.⁴⁴ rAAV2/7 vectors containing either the CMV or enhanced synapsin1 promoter were normalized for GC and injected in the SN (1.1×10^{11} GC ml⁻¹, injected titer 3.3×10^8 GC per animal). *In vivo* BLI at 2 and 5 weeks revealed similar stable transgene expression for both promoters, with a slightly higher signal for the enhanced synapsin1 promoter (Figure 4a). IHC staining for eGFP 6 weeks after injection showed no significant differences in expression pattern (Figure 4b) either in transduced brain volume or in the number of transduced

cells in the SN ($P > 0.05$), but again the enhanced synapsin1 promoter performed slightly better (Figures 4c and d).

Retrograde transport of rAAV vectors after injection into the nigrostriatal pathway

For disease modeling and gene therapy applications, administration of rAAV vectors in the striatum followed by retrograde transport to the SN is an attractive option because of the accessibility of the striatum, explaining its use in current clinical trials. After intranigral injection of different rAAV vectors, we observed widespread anterograde eGFP labeling of projection fibers towards the striatum, with minimal labeling of cell bodies in the striatum (data not shown). To assess the efficiency of retrograde transport towards the DN of the SNpc, the different serotypes were injected into the striatum. All the vectors were injected into the striatum at a higher dose than for the SN injections ($1.0\text{--}5.0 \times 10^{11}$ GC ml⁻¹, injected titer $3.0 \times 10^8\text{--}1.5 \times 10^9$ GC per animal, except 1.0×10^{10} GC ml⁻¹ for rAAV 2/2) (Figure 5a). To analyze the transduced cell type of each rAAV serotype in the striatum, triple staining for eGFP, the neuronal marker NeuN and GFAP was performed (Figure 5b). Detailed confocal microscopic analysis in the transduced region showed a good co-localization of eGFP and NeuN, but not with GFAP for all serotypes tested. This indicates that mainly neurons and not astrocytes were transduced. Numerous eGFP-positive projections in the SN were detected (Figure 5c). In-depth analysis indicated that for all serotypes tested, except for rAAV 2/5, mainly the neurites of the substantia nigra pars reticulata expressed eGFP, while only a minimal number of cell bodies (<1%) in the SNpc tested positive (Figure 5d). However, after intrastriatal injection of rAAV 2/5 we observed 30% of the DN transduced in the SNpc. Thus, of all serotypes tested, only rAAV 2/5 induced substantial transgene expression in the DN of the SN after striatal injection. For rAAV 2/2

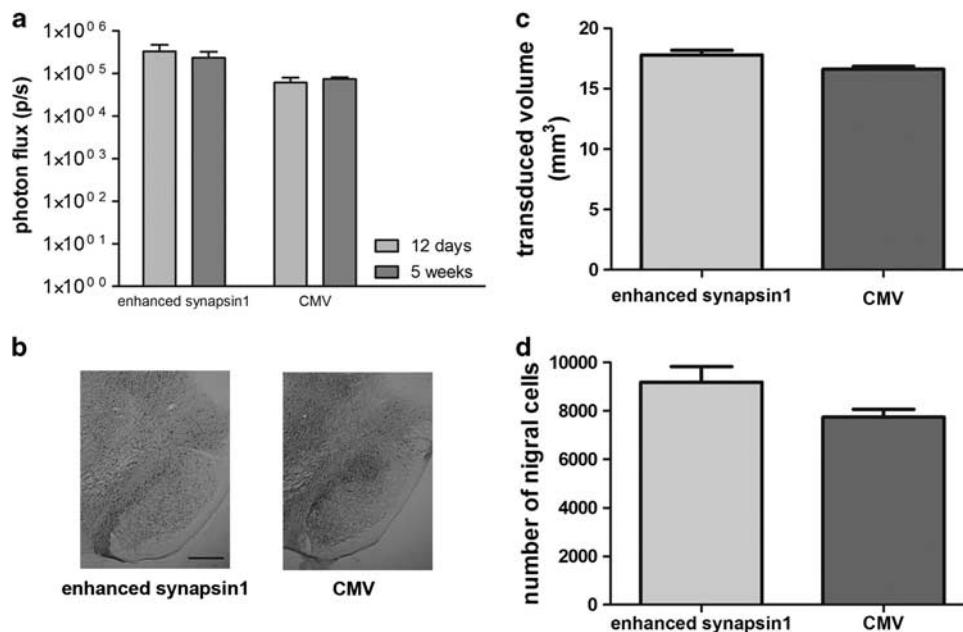


Figure 4 Comparison of the CMV and the enhanced synapsin1 promoter *in vivo*. (a) *In vivo* BLI quantification of fLuc transgene expression in the rat brain. fLuc activity was measured 12 days and 5 weeks after stereotactic injection of both rAAV 2/7 containing either the CMV or the enhanced synapsin1 promoter. The BLI signal observed was comparable for both vectors (mean \pm s.d., $P > 0.05$, $n=5$). (b) IHC staining for eGFP 6 weeks after rAAV 2/7 injection containing either the CMV or the enhanced synapsin1 promoter. Scale bar=400 μ m. (c) Quantification of the expression volume. Equivalent volumes were observed for both promoters (mean \pm s.d., $P > 0.05$, $n=5$). (d) Quantification of the number of eGFP-positive nigral cells in the SN. The number of eGFP-positive nigral cells was similar for both promoters (mean \pm s.d., $P > 0.05$, $n=5$).

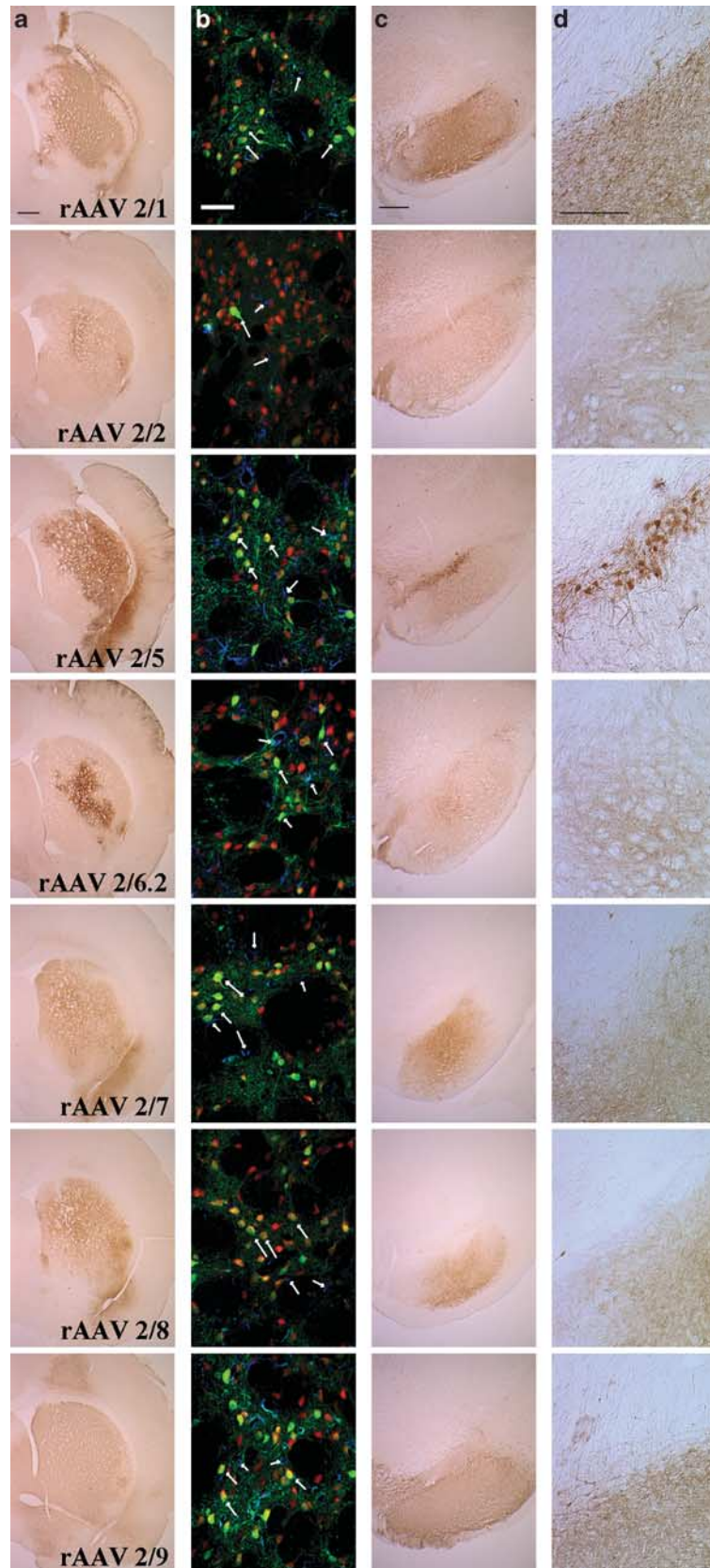


Figure 5 Retrograde transport after injection of rAAV serotypes in the striatum. (a) IHC analysis of eGFP expression in the striatum after intrastratial injection of different serotypes. Scale bar=400 μm , $n=3$. (b) Confocal images of fluorescent triple immunostainings for eGFP, NeuN and GFAP show extensive co-localization of eGFP and NeuN in the transduced region. Arrows mark the transduced neurons and the non-transduced astrocytes. Scale bar=50 μm . (c) Immunostaining for eGFP in the SN after intrastratial injection. Scale bar=400 μm . (d) Detailed image of the SN. Scale bar=200 μm .

we cannot draw final conclusions, as the injected titers we obtained with both production methods did not reach the level of the other serotypes.

Biodistribution of the transgene after high-titer rAAV injection in the brain

To assess the biodistribution of rAAV after stereotactic injection in the CNS, both rats and mice were examined. At 4 weeks after bilateral injection of high-titer (5.0×10^{13} GC ml⁻¹, injected titer 1.5×10^{11} GC per animal) rAAV 2/7 (left) and rAAV2/8 (right) in the striatum of mice, two BLI signals were detected. One signal originated from the site of injection in the brain, the second one from the abdomen (Figure 6a). *Ex vivo* BLI revealed that this ectopic signal arose from the liver. Other organs such as the lung, kidney, heart, spleen, gut and testis were negative in BLI measurements. These observations were quantitatively confirmed by a luciferase assay (Figure 6b). Mice injected with a lower titer (5.0×10^{11} GC ml⁻¹, injected titer 1.5×10^9 GC per animal) rAAV 2/7 (left) and rAAV2/8 (right) in the striatum showed no abdominal signal (Figure 6c). To further determine whether the signal in the mice originated from rAAV 2/7 or rAAV 2/8, both vectors were injected unilaterally into the striatum. Injection of both vectors resulted in a liver signal, but the signal from rAAV 2/7 was much higher compared with rAAV 2/8 (Figure 6e). Next we wanted to verify if this signal also appeared in the rat after bilateral injection of high titers of rAAV 2/7 and rAAV 2/8. As the standard method of rat SN scanning does not include visualization of the abdomen of the rat, we extracted the liver from rats injected in the SN with the high or low titer of vector and performed a luciferase assay. All extracts were negative (Figure 6d).

DISCUSSION

Recombinant AAV vectors are derived from non-pathogenic viruses; they result in long-term transgene expression and are capable of transducing non-dividing cells.⁴⁵ These properties make them attractive agents for gene delivery in the brain, in the context of both disease modeling and gene therapy applications. Several recently discovered rAAV serotypes have gained significant interest because of their transduction efficiency, tropism and less prevalent pre-existing immunity.³⁸ It has become clear that the production and purification method, as well as the addition of functional control elements in the vector genome, can influence rAAV vector tropism, transduction and expression efficiency.^{46,47} Some rAAV serotypes have previously been tested for their ability to transduce DNs in the SN.^{27,28,30} In our study, we performed an extensive comparative analysis of seven different serotypes in the adult rat SN. In contrast to the previous studies, we combined non-invasive imaging and IHC to quantify transgene expression over time, and evaluated the dopaminergic specificity and biodistribution of the vector after local injection.

All seven rAAV serotypes were able to transduce the SN, but differences were observed in terms of expression levels, transduced brain volume and dopaminergic specificity. Overall transgene expression levels were determined by both *in vivo* BLI and histological quantification of transduced brain volume. To make a fair comparison of all serotypes with rAAV 2/2, we produced this serotype once from the supernatant and once from the cell lysate (Supplementary Figure S2), as it has been shown that production of rAAV 2/2 is more efficient from cell lysates.^{40–42} The highest BLI signal was observed with rAAV 2/7, which was 10 times higher compared with rAAV 2/9 and 2/1, whereas rAAV 2/8, 2/5, 2/6.2 and 2/2 resulted in a significantly lower BLI signal. For all serotypes tested, no significant differences in transgene expression levels were detected between

2 and 5 weeks after injection. Therefore, we conclude that the transgene expression remains stable over time and reaches its maximum expression level at or before 2 weeks post transduction. Stable gene expression after rAAV transduction is in accordance with the literature; the differences described in the onset of transgene expression between different serotypes refer to earlier time points (4–7 days).⁴⁸ Using unbiased stereological quantification, we demonstrated that the transduced brain volume with rAAV 2/7, 2/9 and 2/1 was comparable and significantly higher than with rAAV 2/8, 2/5, 2/6.2 and 2/2. The more widespread transgene expression pattern in rat SN with rAAV 2/1 in comparison with rAAV 2/5 has been described before.²⁸ We extend this conclusion to rAAV 2/7 and 2/9.

Analysis of the transduction specificity or vector tropism revealed that rAAV 2/7, 2/9, 2/1 and 2/8 transduced a higher number of nigral cells compared to rAAV 2/5, 2/6.2 and 2/2. For all serotypes tested, the number of transduced nigral cells correlated with the transduced volume, except for rAAV 2/8. Despite a lower transduced brain volume, rAAV 2/8 transduced a high number of nigral cells. This localized expression pattern after injection of rAAV 2/8 might be due to a less widespread diffusion of the vector and/or a higher tropism for DNs. Burger *et al.*²⁸ found that after injection of rAAV 2/1 in the SN of the rat, the number of transduced cells in the entire midbrain was higher than with rAAV 2/5, but when performing stereological cell counts specifically in the SN, these differences were no longer detected. This could be explained by the fact that high rAAV vector titers (3.0×10^{13} GC ml⁻¹) were injected, which may result in saturated expression levels in a small nucleus like the SN. We specifically opted to use low rAAV vector titers (1.0×10^{10} GC ml⁻¹) to adequately compare all serotypes in non-saturating conditions. To further specify the tropism of each serotype specifically for the dopaminergic nigral neurons, extensive analysis and quantification was performed with confocal microscopy. Serotypes 2/7, 2/9, 2/1 and 2/8 transduced the largest number of DNs in the transduced region (>70%), which was significantly higher than with rAAV 2/5 and 2/6.2 (49%). In contrast, McFarland *et al.*³⁰ found no significant differences either in the number of eGFP-positive nigral cells or in the percentage of transduced DNs when comparing rAAV 2/1, 2/5 and 2/8. Their results could be explained by differences in functional control elements in the vector genome, like the absence of the WPRE (woodchuck post-transcriptional regulatory element), or the production and purification method used. Also, the overall percentage of transduced DNs in their study was lower (maximum 50%) than in this study (maximum 80%). There is evidence that the use of optimized production and purification methods increases the vector purity and potency,^{46,47} which might explain the differences in transduction efficiency. However, although some of the serotypes transduced a limited volume or number of target cells with the titers used in this study, they could still prove very useful *in vivo* when used at higher titers. Different groups have studied the transduction efficiency and tropism of novel rAAV serotypes in specific brain regions of different species of animals. These studies show that more recently discovered serotypes are as good as and often better than AAV 2/2 in transducing certain brain regions, and serve as good alternatives.⁴⁹ The discrepancy between some studies made it also clear that it is not always possible to extrapolate findings between different species.^{49,50}

For the design of a specific animal model or for the evaluation of gene therapy applications, the specificity toward a particular cell type can be important. In this context, not only the choice of the serotype but also that of the promoter might have an important role. Furthermore, viral promoters such as the CMV promoter have been shown to be inactivated over time,⁵¹ probably by methylation and/or

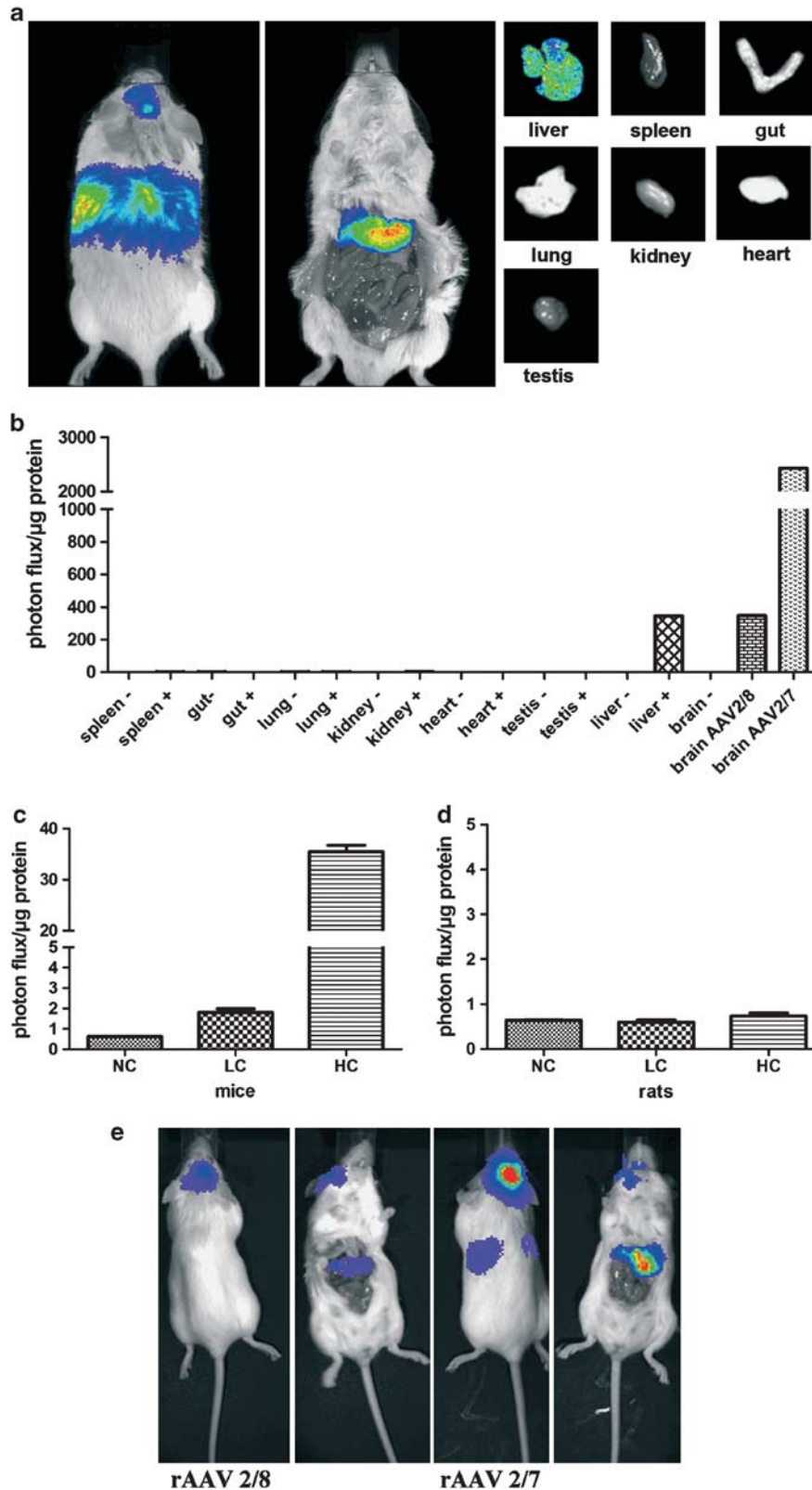


Figure 6 Biodistribution of transgene after high-titer rAAV injection in the brain. (a) BLI signal in overlay with a photographic image of the animal. Four weeks after bilateral injection of rAAV 2/7 and 2/8 into the striatum of mice, two light signals were detected, one signal originating from the brain and another one from the abdomen ($n=3$). *Ex vivo* BLI was performed to assess the origin of the second signal. (b) *Ex vivo* luciferase assay on different organs of high-titer rAAV injected mice ($n=3$). (c) *Ex vivo* luciferase assay on the liver of mice injected with high- (HC) or low-titer (LC) rAAV vector ($n=3$). NC=negative control. (d) *Ex vivo* luciferase assay on the liver of rats injected with high- or low-titer rAAV vector ($n=3$). NC=negative control. (e) BLI signal in overlay with a photographic image of animals after unilateral injection of rAAV 2/7 or rAAV 2/8 in mouse striatum.

histone deacetylation of promoter sequences by the defense machinery of the host cell. Cellular/eukaryotic promoters less likely activate the defense machinery, and thus are usually less sensitive to promoter silencing compared with viral promoters. In addition to the CMV promoter, we expressed identical transgenes under control of the enhanced neuron-specific synapsin1 promoter in an AAV 2/7 serotype. The human synapsin1 promoter has been extensively characterized and its 495-bp 5' flanking region has been shown to drive neuron-specific expression in various regions of the brain.^{43,44} *In vivo* BLI at 2 and 5 weeks revealed similar stable transgene expression for both promoters. IHC analysis showed that both promoters are equal in terms of transduced brain volume and dopaminergic specificity. These data show that the enhanced synapsin1 promoter can be used as a good alternative for the CMV promoter. Comparison of long-term expression and/or silencing with both promoters will require follow-up studies.

The biodistribution and possible ectopic expression of a viral vector after local injection have major implications for the animal model, the biosafety and immune reactions. A viral vector with the ability for retrograde transport is expected to facilitate surgical interventions, as it can be delivered into the striatum and can circumvent direct injection into the SN. Although we observed retrograde transport for all the serotypes tested, only rAAV 2/5 induced substantial transgene expression in the DNs of the SNpc after striatal injection. Our results confirm previous reports on retrograde transduction of DNs in the SNpc with rAAV 2/5.^{27,28,48} Further characterization and titer optimization of rAAV 2/5 will be required to confirm this route as a genuine alternative administration route to target rat DNs.

Unexpectedly, after injection of very high doses of rAAV 2/7 and rAAV 2/8 (5.0×10^{13} GC ml⁻¹, 1.5×10^{11} GC per animal) in mouse brain, substantial transduction was observed systemically, mostly from the liver, which highlights the risk of systemic dissemination of vector after local injection in mouse striatum. This phenomenon, however, was never observed in rat, suggesting that species specificity or factors related to scale have a role in this phenomenon. It also means that stereotactic injection of very-high-titer rAAV preparations in the brain can result in both local toxicity and systemic dissemination of vector particles. The latter can have repercussions on the immune-privileged status of the CNS with regard to transgene expression and unwanted immune responses. The use of a more specific promoter like the enhanced synapsin1 promoter may prevent transgene expression in peripheral cell types.

In conclusion, rAAV vectors with high transduction efficiency are very valuable in the context of both gene therapy and disease modeling. This study was primarily carried out in light of the further development of a viral vector-mediated rat model for PD. For this application, rAAV 2/7, 2/9, 2/1 and 2/8 performed best, with rAAV 2/7 being superior in terms of overall transgene expression levels. rAAV 2/8 resulted in lower overall transgene expression levels and transduced brain volume, but the vector performed equally well at the level of the number of transduced DNs in the SN. Thus, rAAV 2/8 might be the vector of choice for specific targeting of the SN. Our results facilitate the design and selection of rAAV vector serotypes for transduction of DNs in the SNpc, and the refinement of the viral vector-based rat model for PD. In addition, our data are relevant to the use and design of rAAV gene therapy strategies in the CNS.

MATERIALS AND METHODS

Cloning of AAV plasmids

The plasmids for the recombinant rAAV vector production were described previously.⁵² These plasmids include the constructs for the different serotypes

(AAV 2/1, 2/2, 2/5, 2/6.2, 2/7, 2/8 and 2/9), the AAV transfer plasmid (pZac 2.1 eGFP3 SEED) encoding the eGFP transgene under the control of the ubiquitous CMV promoter and the pAdvDeltaF6 adenoviral helper plasmid. The AAV transfer plasmid with the AAV2 terminal repeats (ITR) flanking the CMV promoter–GFP–WPRE–bovine growth hormone polyadenylation sequence was modified to include both eGFP and fluc as transgenes under the control of the CMV promoter. Initially, the eGFP transgene was replaced by a multiple cloning site inserted between the *NotI* and *BamHI* site in the original transfer plasmid. Into this multiple cloning site the eGFP–T2A–fluc sequence was cloned, encoding both eGFP and fluc separated by the 2A peptide sequence, which allows a bicistronic expression of both proteins from the same mRNA.⁵³ This construct will further be referred to as the transfer plasmid. For the comparison of the promoters *in vivo*, the CMV promoter was replaced by the CMVie-enhanced synapsin1 promoter.

Serum-free recombinant rAAV production

Subconfluent, low (<50) passage adherent HEK 293T cells (ATCC, Manassas, VA, USA) were transfected using a 25-kDa linear polyethylenimine solution using the AAV-TF, AAV rep/cap and pAdbDeltaF6 plasmids in the ratio of 1:1:1. Productions were performed using a Hyperflask Cell Culture Vessel (1720 cm² growth area, Corning Life Sciences, Kennebunk, ME, USA). 293T cells were seeded in the Hyperflask at 1×10^8 cells per production in Optimem (Invitrogen, Merelbeke, Belgium) with 2% fetal calf serum. The next day, 400 µg of pAAV-TF plasmid, 400 µg of rep/cap construct and 400 µg of pAdbDeltaF6 plasmid were mixed in 20 ml of 150 mM NaCl. An equal volume containing 4 ml of 10 mM polyethylenimine solution and 16 ml of 150 mM NaCl was added slowly to the DNA mixture. Following 15 min incubation at room temperature, the DNA–polyethylenimine complex was added to the 293T cells in Optimem with 0% fetal calf serum. After 24 h of incubation at 37 °C in a 5% CO₂ humidified atmosphere, the medium was replaced with Optimem with 0% fetal calf serum. The supernatant was harvested 3 days after transient transfection and concentrated using tangential flow filtration.

Recombinant rAAV purification

The concentrated supernatant was purified using an iodixanol step gradient. Iodixanol was diluted with phosphate-buffered saline (PBS) containing a final concentration of 1 M NaCl in the 20, 30 and 40% (w/v) solutions. A discontinuous gradient was made by carefully underlayering the concentrated supernatant with 5 ml of 20% iodixanol, 3 ml of 30% iodixanol, 3 ml of 40% iodixanol and 3 ml of 60% iodixanol. The gradient was centrifuged in a Beckman Ti-70 fixed angle rotor (Analis, Gent, Belgium) at 27 000 r.p.m. for 2 h. Gradient fractions were collected in 250-µl aliquots and all fractions with a Refraction Index between 1.39 and 1.42 were pooled. The pooled fractions were centrifuged in a Vivaspin 6 (PES, 100,000 MWCO, Sartorius AG, Goettingen, Germany) using a swinging bucket rotor at 3000 g. The iodixanol of the pooled fractions was exchanged five times with PBS using this procedure. The final sample was aliquoted and stored at –80 °C. Characterization of the rAAV stocks included real-time PCR analysis for genomic copy determination and silver-stained sodium dodecyl sulfate–polyacrylamide gel electrophoresis (SDS–PAGE) analysis for vector purity. Briefly, real-time PCR was performed using a primer probe set for the polyA sequence (primer sequences, 5'-TCTAGTTGCCAGCCATCTGTTGT-3' and 5'-TGGGAGTGGCACCTTC CA-3'; probe sequence, 5'-TCCCCCGTGCTTCCTTGACC-3'). Genome copies obtained for the different productions ranged between 1×10^{10} and 3×10^{13} GC ml⁻¹.

Stereotactic injections

All animal experiments were carried out in accordance with the European Communities Council Directive of 24 November 1986 (86/609/EEC) and approved by the Bioethical Committee of the KULeuven (Belgium). Young adult female Wistar rats (Janvier, Le-Genest-Saint-Isle, France) weighing about 200–250 g and young adult female C57BL/6J–*Tyr^{c-2}/J* mice (Jackson Laboratory, Bar Harbor, ME, USA) weighing about 25 g were housed under a normal 12-h light/dark cycle with free access to pelleted food and tap water. All surgical procedures were performed using aseptic techniques and ketamine (60 mg kg⁻¹ i.p. (rat) and 75 mg kg⁻¹ i.p. (mice), Ketalar, Pfizer, Puurs,

Belgium) and medetomidine (0.4 mg kg⁻¹ (rat) and 1 mg kg⁻¹ (mice), Dormitor, Pfizer, Belgium) anesthesia. Following anesthesia, the rodents were placed in a stereotactic head frame (Stoelting, Wood Dale, IL, USA). Injections were performed with a 30-gauge needle and a 10- μ l Hamilton syringe. All animals were injected with 3 μ l vector. Stereotactic coordinates used for the SN of the rat were anteroposterior (AP) -5.3, lateral (LAT) -2.0 and dorsoventral (DV) -7.2, calculated from the dura using bregma as reference. Coordinates used for the striatum of the rat were AP 0, LAT -2.0 and DV -5.5, and for the striatum of the mouse AP +0.5, LAT -2.0 and DV -3.0. The injection rate was 0.25 μ l min⁻¹; the needle was left in place for an additional 5 min before being retracted.

In vivo bioluminescence imaging

The animals were anesthetized and imaged in an IVIS 100 system (Caliper Life Sciences, Hopkinton, MA, USA) as described previously.⁵⁴ The animals were injected with D-luciferin (126 mg kg⁻¹, Promega, Benelux, Leiden, The Netherlands) dissolved in PBS (rats: 30 mg ml⁻¹, mice: 15 mg ml⁻¹) in the lateral tail vein (rats) or intraperitoneal region (mice). Subsequently, they were placed in the prone position in the IVIS and frames were acquired with a field of view of 10 cm (rats) or 20 cm (mice). Consecutive scans with an acquisition time of 1 min were performed until the maximal signal was reached. For the quantification of rAAV gene activity *in vivo*, the data are reported as total photon flux (p/s) from a 3.0-cm² circular region of interest on the head. For *ex vivo* BLI, the animals were killed, the organs dissected and BLI scans performed with an acquisition time of 1 min.

Histology

Six weeks after rAAV vector injection, rats were killed with an overdose of sodium pentobarbital (60 mg kg⁻¹, i.p., Nembutal, Ceva Santé, Belgium) followed by intracardial perfusion with 4% paraformaldehyde in PBS. After postfixation overnight, 50- μ m-thick coronal brain sections were made with a vibrating microtome (HM 650V, Microm, Walldorf, Germany). IHC was performed on free-floating sections using an in-house antibody raised against eGFP (rabbit polyclonal 1:10 000). Sections were pretreated with 3% hydrogen peroxide for 10 min and incubated overnight with primary antibody in 10% normal swine serum (DakoCytomation, Heverlee, Belgium). As secondary antibody, we used biotinylated anti-rabbit IgG (1:300, DakoCytomation), followed by incubation with streptavidin-horseradish peroxidase complex (DakoCytomation). eGFP immunoreactivity was visualized using 3,3'-diaminobenzidine (0.4 mg ml⁻¹, Sigma-Aldrich, Bornen, Belgium) as a chromogen.

For fluorescent double staining, sections were rinsed thrice in PBS and then incubated overnight in PBS-0.1% triton X-100, 10% goat serum, rabbit anti-eGFP (1:1000, in-house) and mouse anti-TH (1:1000, Chemicon, Millipore, Brussels, Belgium). After three rinses in PBS-0.1% triton X-100, the sections were incubated in the dark for 1 h in fluorochrome-conjugated secondary antibodies: goat anti-rabbit Alexa 488 (1:500, Molecular Probes, Invitrogen, Merelbeke, Belgium) and goat anti-mouse Alexa 633 (1:500, Molecular Probes, Invitrogen). After being rinsed in PBS and mounted, the sections were coverslipped with mowiol. For triple staining, the same protocol was applied using chicken anti-eGFP (1:500, Aves Lab Inc., Tigard, OR, USA), rabbit anti-GFAP (1:100, Dako, Heverlee, Belgium) and mouse anti-TH (1:1000, Chemicon) or mouse anti-NeuN (1:500, Chemicon) as primary antibodies. Secondary antibodies were donkey anti-chicken FITC (1:500, Jackson IMRL, Newmarket, UK), donkey anti-rabbit Alexa 555 (1:500, Molecular Probes, Invitrogen) and donkey anti-mouse Alexa 633 (1:500, Molecular Probes, Invitrogen).

Stereological quantification

The volume of eGFP-immunoreactive neurons and fibers in the brain was determined by stereological volume measurements using the Cavalieri method in a computerized system as described before⁵⁵ (StereoInvestigator; MicroBright-Field, Magdeburg, Germany). Every fifth section covering the entire extent of the SN, with a total of eight sections for each animal, was included in the counting procedure. The coefficients of error, calculated according to the procedure of Schmitz and Hof as estimates of precision,⁵⁶ varied between 0.05 and 0.14. The number of eGFP-positive cells in the SN was

estimated using an optical fractionator sampling design.⁵⁶ Every fifth section throughout the entire SN was analyzed, with a total of eight sections for each animal. The coefficients of error varied between 0.05 and 0.10.

Confocal microscopy

GFP and TH- or GFAP-positive cells were visualized by confocal microscopy with an LSM 510 unit (magnification $\times 40$, Zeiss, Zaventem, Belgium). Three sections with a 250- μ m interval were selected from the site of injection. A minimum of 120 GFP⁺/TH⁺ cells were counted and the percentage GFP⁺/TH⁺ relative to the total TH⁺ population was determined.

Ex vivo luciferase enzyme activity assay

Animals were killed 4 weeks after injection. All the different organs were snap frozen in liquid nitrogen, homogenized and subsequently lysed with 1 ml of lysis buffer containing 50 mM Tris (pH 7.5), 200 mM NaCl, 0.2% Nonidet P-40, 1 mM phenylmethylsulfonyl fluoride and 10% glycerol. After lysis, samples were immediately centrifuged at 13 000 g for 1 min. Twenty microliters of the supernatant was assayed for luciferase activity according to the manufacturer's protocol (ONE-Glo luciferase assay system; Promega, Madison, WI, USA) and the light produced was measured at an integration time of 3 s with a GloMax luminometer (Promega). Data were normalized to the total protein concentration, which was determined by the bicinchoninic acid assay (Pierce Biotechnology, Rockford, IL, USA).

Statistical analysis

For each serotype, the mean transduced volume and the mean transduction efficiency in DN_s were compared using one-way analysis of variance followed by Bonferroni *post-hoc* testing. To compare the total number of nigral cells, we used one-way analysis of variance followed by Tukey *post-hoc* test. *In vivo* BLI quantification of fLuc transgene expression was compared using a non-parametric Kruskal-Wallis test followed by Dunn's *post-hoc* testing. Statistical analysis was performed using GraphPad Prism. Statistical significance level was set as follows: **P* < 0.05, ***P* < 0.01, ****P* < 0.001.

CONFLICT OF INTEREST

LHV holds patents on the technology described within. JMW is an inventor on patents licensed to various biopharmaceutical companies, including ReGenX, for which he has equity in, consults for and receives a grant from.

ACKNOWLEDGEMENTS

We thank Martine Michiels and Phebe van Wijk for their excellent technical assistance. AVdP, JT and MC are doctoral fellows supported by grants from the Institute for the Promotion of Innovation through Science and Technology in Flanders (IWT-Vlaanderen). BH is a doctoral fellow supported by a grant from the Flemish Fund for Scientific Research (FWO-Vlaanderen). Research was funded by the IWT-Vlaanderen (IWT SBO/060838 and IWT SBO/80020), by the EC-FP6 program 'DiMI' (LSHB-CT-2005-512146), the FP7 RTD project MEFOPA (HEALTH-2009-241791), the KULeuven (IOF-KP/07/001 and OT/08/052A), the Interuniversity Attraction Pole programme NiMI (P6/38) and the KULeuven Center of Excellence 'MoSAIC' (EF/05/08). Confocal images were taken in the cell imaging core of the KULeuven.

- Jain S, Wood NW, Healy DG. Molecular genetic pathways in Parkinson's disease: a review. *Clin Sci (Lond)* 2005; **109**: 355-364.
- Lesage S, Brice A. Parkinson's disease: from monogenic forms to genetic susceptibility factors. *Hum Mol Genet* 2009; **18**: R48-R59.
- Gasser T. Mendelian forms of Parkinson's disease. *Biochim Biophys Acta* 2009; **1792**: 587-596.
- Hardy J, Cai H, Cookson MR, Gwinn-Hardy K, Singleton A. Genetics of Parkinson's disease and parkinsonism. *Ann Neurol* 2006; **60**: 389-398.
- Gasser T. Molecular pathogenesis of Parkinson disease: insights from genetic studies. *Expert Rev Mol Med* 2009; **11**: e22.
- Kirik D, Rosenblad C, Burger C, Lundberg C, Johansen TE, Muzyczka N *et al*. Parkinson-like neurodegeneration induced by targeted overexpression of alpha-synuclein in the nigrostriatal system. *J Neurosci* 2002; **22**: 2780-2791.

- 7 Eslamboli A, Romero-Ramos M, Burger C, Bjorklund T, Muzyczka N, Mandel RJ *et al*. Long-term consequences of human alpha-synuclein overexpression in the primate ventral midbrain. *Brain* 2007; **130**: 799–815.
- 8 Kirik D, Annett LE, Burger C, Muzyczka N, Mandel RJ, Bjorklund A. Nigrostriatal alpha-synucleinopathy induced by viral vector-mediated overexpression of human alpha-synuclein: a new primate model of Parkinson's disease. *Proc Natl Acad Sci USA* 2003; **100**: 2884–2889.
- 9 Lauwers E, Debysers Z, Van Dorpe J, De Strooper B, Nuttin B, Baekelandt V. Neuro-pathology and neurodegeneration in rodent brain induced by lentiviral vector-mediated overexpression of alpha-synuclein. *Brain Pathol* 2003; **13**: 364–372.
- 10 Klein RL, King MA, Hamby ME, Meyer EM. Dopaminergic cell loss induced by human A30P alpha-synuclein gene transfer to the rat substantia nigra. *Hum Gene Ther* 2002; **13**: 605–612.
- 11 Manfredsson FP, Burger C, Sullivan LF, Muzyczka N, Lewin AS, Mandel RJ. rAAV-mediated nigral human parkin over-expression partially ameliorates motor deficits via enhanced dopamine neurotransmission in a rat model of Parkinson's disease. *Exp Neurol* 2007; **207**: 289–301.
- 12 Vercammen L, Van der Perren A, Vaudano E, Gijsbers R, Debysers Z, Van den Haute C *et al*. Parkin protects against neurotoxicity in the 6-hydroxydopamine rat model for Parkinson's disease. *Mol Ther* 2006; **14**: 716–723.
- 13 Winklhofer KF. The parkin protein as a therapeutic target in Parkinson's disease. *Expert Opin Ther Targets* 2007; **11**: 1543–1552.
- 14 Kirik D, Rosenblad C, Bjorklund A. Characterization of behavioral and neurodegenerative changes following partial lesions of the nigrostriatal dopamine system induced by intraatrial 6-hydroxydopamine in the rat. *Exp Neurol* 1998; **152**: 259–277.
- 15 Jenner P, Rupniak NM, Rose S, Kelly E, Kilpatrick G, Lees A *et al*. 1-Methyl-4-phenyl-1,2,3,6-tetrahydropyridine-induced parkinsonism in the common marmoset. *Neurosci Lett* 1984; **50**: 85–90.
- 16 Hoglinger GU, Oertel WH, Hirsch EC. The rotenone model of parkinsonism—the five years inspection. *J Neural Transm Suppl* 2006; **70**: 269–272.
- 17 Thiruchelvam M, Brockel BJ, Richfield EK, Baggs RB, Cory-Slechta DA. Potentiated and preferential effects of combined paraquat and maneb on nigrostriatal dopamine systems: environmental risk factors for Parkinson's disease? *Brain Res* 2000; **873**: 225–234.
- 18 Fleming SM, Fernagut PO, Chesselet MF. Genetic mouse models of parkinsonism: strengths and limitations. *NeuroRx* 2005; **2**: 495–503.
- 19 Freichel C, Neumann M, Ballard T, Muller V, Woolley M, Ozmen L *et al*. Age-dependent cognitive decline and amygdala pathology in alpha-synuclein transgenic mice. *Neurobiol Aging* 2007; **28**: 1421–1435.
- 20 Goldberg MS, Fleming SM, Palacino JJ, Cepeda C, Lam HA, Bhatnagar A *et al*. Parkin-deficient mice exhibit nigrostriatal deficits but not loss of dopaminergic neurons. *J Biol Chem* 2003; **278**: 43628–43635.
- 21 Itier JM, Ibanez P, Mena MA, Abbas N, Cohen-Salmon C, Bohme GA *et al*. Parkin gene inactivation alters behaviour and dopamine neurotransmission in the mouse. *Hum Mol Genet* 2003; **12**: 2277–2291.
- 22 Kahle PJ. alpha-Synucleinopathy models and human neuropathology: similarities and differences. *Acta Neuropathol* 2008; **115**: 87–95.
- 23 Ulusoy A, Bjorklund T, Hermening S, Kirik D. In vivo gene delivery for development of mammalian models for Parkinson's disease. *Exp Neurol* 2008; **209**: 89–100.
- 24 Lo Bianco C, Ridet JL, Schneider BL, Deglon N, Aebischer P. (alpha)-Synucleinopathy and selective dopaminergic neuron loss in a rat lentiviral-based model of Parkinson's disease. *Proc Natl Acad Sci USA* 2002; **99**: 10813–10818.
- 25 Lo Bianco C, Schneider BL, Bauer M, Sajadi A, Brice A, Iwatsubo T *et al*. Lentiviral vector delivery of parkin prevents dopaminergic degeneration in an alpha-synuclein rat model of Parkinson's disease. *Proc Natl Acad Sci USA* 2004; **101**: 17510–17515.
- 26 Schneider B, Zufferey R, Aebischer P. Viral vectors, animal models and new therapies for Parkinson's disease. *Parkinsonism Relat Disord* 2008; **14**(Suppl 2): S169–S171.
- 27 Paterna JC, Feldon J, Bueler H. Transduction profiles of recombinant adeno-associated virus vectors derived from serotypes 2 and 5 in the nigrostriatal system of rats. *J Virol* 2004; **78**: 6808–6817.
- 28 Burger C, Gorbatyuk OS, Velardo MJ, Peden CS, Williams P, Zolotukhin S *et al*. Recombinant AAV viral vectors pseudotyped with viral capsids from serotypes 1, 2, and 5 display differential efficiency and cell tropism after delivery to different regions of the central nervous system. *Mol Ther* 2004; **10**: 302–317.
- 29 Taymans JM, Vandenberghe LH, Haute CV, Thyry I, Deroose CM, Mortelmans L *et al*. Comparative analysis of adeno-associated viral vector serotypes 1, 2, 5, 7, and 8 in mouse brain. *Hum Gene Ther* 2007; **18**: 195–206.
- 30 McFarland NR, Lee JS, Hyman BT, McLean PJ. Comparison of transduction efficiency of recombinant AAV serotypes 1, 2, 5, and 8 in the rat nigrostriatal system. *J Neurochem* 2009; **109**: 838–845.
- 31 Dodiya HB, Bjorklund T, Stansell III J, Mandel RJ, Kirik D, Kordower JH. Differential transduction following basal ganglia administration of distinct pseudotyped AAV capsid serotypes in nonhuman primates. *Mol Ther* 2009; **18**: 579–587.
- 32 Blits B, Derks S, Twisk J, Ehler E, Prins J, Verhaagen J. Adeno-associated viral vector (AAV)-mediated gene transfer in the red nucleus of the adult rat brain: comparative analysis of the transduction properties of seven AAV serotypes and lentiviral vectors. *J Neurosci Methods* 2009; **185**: 257–263.
- 33 Davidson BL, Stein CS, Heth JA, Martins I, Kotin RM, Derksen TA *et al*. Recombinant adeno-associated virus type 2, 4, and 5 vectors: transduction of variant cell types and regions in the mammalian central nervous system. *Proc Natl Acad Sci USA* 2000; **97**: 3428–3432.
- 34 Passini MA, Watson DJ, Wolfe JH. Gene delivery to the mouse brain with adeno-associated virus. *Methods Mol Biol* 2004; **246**: 225–236.
- 35 Gao GP, Alvira MR, Wang L, Calcedo R, Johnston J, Wilson JM. Novel adeno-associated viruses from rhesus monkeys as vectors for human gene therapy. *Proc Natl Acad Sci USA* 2002; **99**: 11854–11859.
- 36 Gao G, Vandenberghe LH, Alvira MR, Lu Y, Calcedo R, Zhou X *et al*. Clades of Adeno-associated viruses are widely disseminated in human tissues. *J Virol* 2004; **78**: 6381–6388.
- 37 Vandenberghe LH, Breous E, Nam HJ, Gao G, Xiao R, Sandhu A *et al*. Naturally occurring singleton residues in AAV capsid impact vector performance and illustrate structural constraints. *Gene Therapy* 2009; **16**: 1416–1428.
- 38 Vandenberghe LH, Wilson JM. AAV as an immunogen. *Curr Gene Ther* 2007; **7**: 325–333.
- 39 Fitzsimons HL, Bland RJ, During MJ. Promoters and regulatory elements that improve adeno-associated virus transgene expression in the brain. *Methods* 2002; **28**: 227–236.
- 40 Vandenberghe LH, Xiao R, Lock M, Lin J, Korn M, Wilson JM. Efficient serotype-dependent release of functional vector into the culture medium during adeno-associated virus manufacturing. *Hum Gene Ther* 2010; **21**: 1251–1257.
- 41 Toelen J, VdP A, Carlon M, Michiels M, Lock M, Vandenberghe L *et al*. *Gene Therapy* submitted.
- 42 Lock M, Alvira M, Vandenberghe LH, Samanta A, Toelen J, Debysers Z *et al*. Rapid, simple, and versatile manufacturing of recombinant adeno-associated viral vectors at scale. *Hum Gene Ther* 2010; **21**: 1259–1271.
- 43 Kugler S, Meyn L, Holzmuller H, Gerhardt E, Iseemann S, Schulz JB *et al*. Neuron-specific expression of therapeutic proteins: evaluation of different cellular promoters in recombinant adenoviral vectors. *Mol Cell Neurosci* 2001; **17**: 78–96.
- 44 Schoch S, Cibelli G, Thiel G. Neuron-specific gene expression of synapsin I. Major role of a negative regulatory mechanism. *J Biol Chem* 1996; **271**: 3317–3323.
- 45 Grimm D, Kay MA. From virus evolution to vector revolution: use of naturally occurring serotypes of adeno-associated virus (AAV) as novel vectors for human gene therapy. *Curr Gene Ther* 2003; **3**: 281–304.
- 46 Ayuso E, Mingozzi F, Montane J, Leon X, Anguela XM, Haurigot V *et al*. High AAV vector purity results in serotype- and tissue-independent enhancement of transduction efficiency. *Gene Therapy* 2009; **17**: 503–510.
- 47 Klein RL, Dayton RD, Tatom JB, Henderson KM, Henning PP. AAV8, 9, Rh10, Rh43 vector gene transfer in the rat brain: effects of serotype, promoter and purification method. *Mol Ther* 2008; **16**: 89–96.
- 48 Reimnsider S, Manfredsson FP, Muzyczka N, Mandel RJ. Time course of transgene expression after intraatrial pseudotyped rAAV2/1, rAAV2/2, rAAV2/5, and rAAV2/8 transduction in the rat. *Mol Ther* 2007; **15**: 1504–1511.
- 49 Markakis EA, Vives KP, Bober J, Leichter S, Leranthe C, Beecham J *et al*. Comparative transduction efficiency of AAV vector serotypes 1–6 in the substantia nigra and striatum of the primate brain. *Mol Ther* 2010; **18**: 588–593.
- 50 Flotte TR, Fischer AC, Goetzmann J, Mueller C, Cebotaru L, Yan Z *et al*. Dual reporter comparative indexing of rAAV pseudotyped vectors in chimpanzee airway. *Mol Ther* 2010; **18**: 594–600.
- 51 Prosch S, Stein J, Staak K, Liebenthal C, Volk HD, Kruger DH. Inactivation of the very strong HCMV immediate early promoter by DNA CpG methylation *in vitro*. *Biol Chem Hoppe Seyler* 1996; **377**: 195–201.
- 52 Gao G, Vandenberghe LH, Wilson JM. New recombinant serotypes of AAV vectors. *Curr Gene Ther* 2005; **5**: 285–297.
- 53 Ibrahim A, Vande Velde G, Reumers V, Toelen J, Thyry I, Vandeputte C *et al*. Highly efficient multicistronic lentiviral vectors with peptide 2A sequences. *Hum Gene Ther* 2009; **20**: 845–860.
- 54 Deroose CM, Reumers V, Gijsbers R, Bormans G, Debysers Z, Mortelmans L *et al*. Noninvasive monitoring of long-term lentiviral vector-mediated gene expression in rodent brain with bioluminescence imaging. *Mol Ther* 2006; **14**: 423–431.
- 55 Baekelandt V, Claeys A, Eggermont K, Lauwers E, De Strooper B, Nuttin B *et al*. Characterization of lentiviral vector-mediated gene transfer in adult mouse brain. *Hum Gene Ther* 2002; **13**: 841–853.
- 56 Schmitz C, Hof PR. Design-based stereology in neuroscience. *Neuroscience* 2005; **130**: 813–831.

Supplementary Information accompanies the paper on Gene Therapy website (<http://www.nature.com/gt>)